DEPOSITION OF VARIOUS SHAPES PARTICLES ON A ROUGH SURFACE IN TURBULENT FLOW

M. Shams

CAE Center, Thermal Mechanics Laboratory, Iran University of Science and Technology
Tehran, Iran mehrzad_shams@yahoo.com

H. Rahimzadeh

Department of Mechanical Engineering, Amirkabir University of Technology
Tehran, Iran, rahimzad@yahoo.com

G. Ahmadi

Department of Mechanical and Aeronautical Engineering, Clarkson University
Potsdam, NY 13699, USA, ahmadi@clarkson

(Received: November 16, 2000 – Accepted in Revised Form: April 9, 2002)

Abstract An experiment set-up is used to study wall deposition rate of particles on a rough surface in a turbulent channel flow. Deposition velocities for three classes of particles, namely, spherical glass particles, irregular shape polymer particles, and fibrous silicon particles are studied. The particle concentration at the test section was measured with the aid of an isokinetic probe in conjunction with a digital image processing technique. The probe is made of sterile plastic and sticked to the sidewall of the wind tunnel. The deposition of spherical particles is found to increase with increasing in diameter. Also it is shown that the deposition velocity of spherical particles is affected by the surface roughness.

Key Word Experimental Two Phase Fluid Flow, Rough or Smooth Surface Aerosol Flow, Turbulent Aerosol Flow

چکیده ته نشینی ذرات بر روی دیواره با سطح زبر در یک کانال با جریان آشفته با استفاده از یک سیستم آزمایشگاهی مورد مطالعه قرار گرفته است. سرعت ته نشینی برای سه دسته از ذرات شیشه ای کروی، ذرات پلیمری با شکل غیر منتظم و ذرات سیلیس فیبری گون بررسی شده است. غلظت ذرات در درون مقطع آزمایش با استفاده از نمونه بردار هم سینتیک و تکنیک پردازش تصویری دیجیتال اندازه گیری شده است. برای تعیین غلظت ذرات ته نشین شده از یک نوار لاستیکی استریل سود جسته شده است. این نوار به دیواره های تونل باد چسبانده شده تا ذرات ته نشین شده بر روی دیواره ها، جمع آوری گردد. اثر زبری سطح بر ته نشینی ذرات کروی مورد مطالعه قرار گرفته است. همچنین ته نشینی ذرات غیر منتظم نیز اندازه گیری شده است. پخش ذرات فیبری گون نیز در تونل باد بررسی شده است.

1. INTRODUCTION

Understanding aerosol transport and deposition processes have received considerable attention due to their numerous industrial and practical applications. Air pollution controls, inhalation toxicology, industrial gas cleaning, and micro-contamination control are among the areas that aerosol transport and deposition plays a critical role. Cooper [1] noted many important applications of particle deposition and removal in microelectronics industry. Fuchs [2], Friedlander [3], Hinds [4,5], Hedley [6] and Vincent [7] reviewed earlier works on aerosol transport and deposition, extensively.

Several authors studied the deposition of particles in vertical tubes, experimentally.

Stavropoulos (1957) used 24.5 μm lycopodium spores to investigate the particle deposition rates on the inside of a vertical glass tube with a petroleum jelly coated wall. Wells and Chamberlain [8] used 0.17-5 μm particles of different densities in their experimental study for a range of Reynolds numbers up to 10^5. The deposition rate was measured for both smooth and rough surface. They found that surface roughness substantially increases the deposition rate. Namie and Ueda [9] measured the deposition rate of water droplets in a horizontal duct. Their results show that the concentration profile were asymmetric, and exhibited a maximum close to the wall for 131-187 μm diameter particles. Also McCoy and Hanratty [10] used 413-617 μm water droplets and found strongly asymmetric concentration profiles. It should be emphasized that for such large particles the inertia diffusion and gravitational settling rather than turbulence are the dominating deposition mechanisms. Montgomery [11] measured droplet concentration in fully developed horizontal turbulent channel flows. Spherical (0.44-2.16 μm) particles were used with a range of Reynolds number between $5*10^3$ and $3.7*10^7$. The experimental study was carried out by Kvasnak et. al [12] to determine the deposition velocity of glass beads and dust particles in turbulence flows in a horizontal duct. They measured the particle deposited onto a flat gold plate covered with a thin film coating. Their results were comparable to other simulations and experimental data.

Only a few works have been reported on the experimental behavior of rigid fibers. Griffiths and Vaughan (1986) checked the aerodynamic behavior of cylindrical and spheroidal particles under gravity. They showed experimentally that the aerodynamical behavior of rigid fibers could be expressed either as straight cylindrical particles or prolate spheroids sedimenting in the direction perpendicular to their polar (major) axis. Shapiro and Goldenberg (1993) developed an experimental technique for measuring the deposition velocities of non-spherical particles from turbulent flow. They measured the deposition velocities of the cylindrical particles of diameters 0.6-2.5 μm and lengths of up to 50 μm. Kvasnak and Ahmadi [13] measured the deposition of rigid fibrous particles in a horizontal wind tunnel. They developed an empirical formula for the deposition efficiency of rigid fibers based on their experimental results.

2. EXPERIMENTAL APPARATUS

Details of the aerosol wind tunnel, the isokinetic sampling probe and the image processing system used in the experiment are described in this section.

Wind Tunnel The aerosol horizontal wind tunnel used in the experiment consists of a rectangular duct with a height of 15.25 cm and 2.54 cm width. The height to width aspect ratio of about six provides a roughly two-dimensional flow condition near the centerline of the channel. The channel is 3.2 m long, and the test section, which is 0.36 m long, is 2.36 m from the inlet contraction section. The tunnel provides a 50 hydraulic diameter needed to ensure a fully developed velocity profile at the test section. The 15.25 cm wall where deposition is measured is oriented vertically to eliminate the effect of gravity on deposition rate. Gravity does not effect deposition on the sidewall of the tunnel where deposition is being measured, however it does not increase the deposition rate on the bottom of the channel and decrease it on the top of the channel. Those surfaces are not considered in this case.

The wind tunnel uses a 11 KW, three phase, ac motor which is connected to a digital voltage inventor. The motor is attached to a blower, which is capable of providing a wide range of test section velocities from 1.3 m/s to over 100 m/s. The blower motor combination sits on a half ton steel reinforced concrete block, and has very little vibration even at exceedingly large rpm. The blower exits into a 0.61 m long diffuser. The sidewalls of the diffuser are at an angle of 4.2 degrees, and the top and bottom walls are at 7.3 degrees. The end of the diffuser contains a HEPA filter 99.9999% efficient in the removal of particles equal to or larger than 0.1 μm in diameter. Particles are injected through the use of a compressed air injector and then pass through a slat system used to mix the particles with the flow and create a homogenous aerosol. A 76 mm long hexagonal aluminum honeycomb with a cell size of 9.5 mm and a series of screens are used to reduce the turbulence caused by the injection of particles before the flow reaches the contraction section. A fifth order contraction section reduces the cross sectional area of the flow by a ninety six to one ratio. The end of the tunnel consists of a diffuser and a final HEPA filter. Figure 1 shows

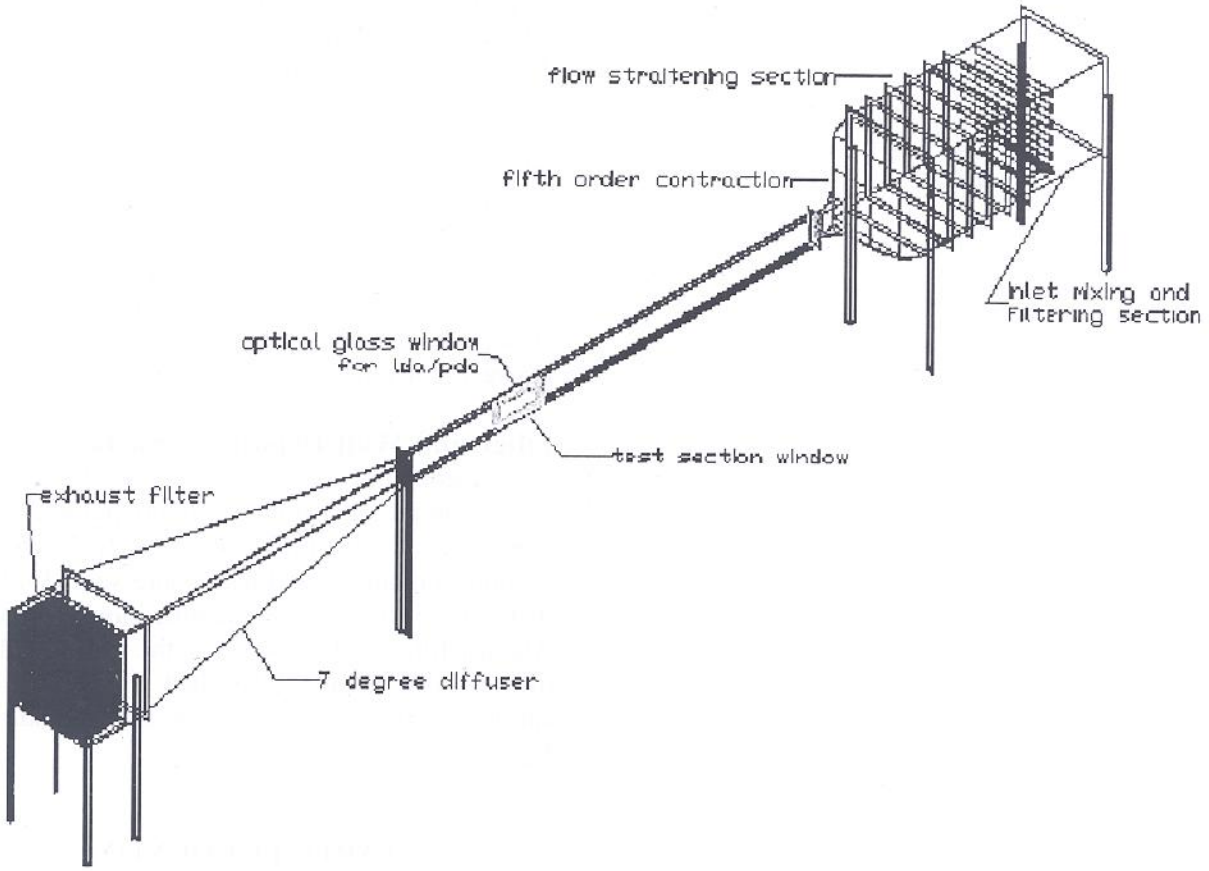

Figure 1. Schematic drawing of the wind tunnel.

the schematic drawing of the wind tunnel. More details of the tunnel are discussed in Kvasnak and Ahmadi [13] and Gayne [14].

Isokinetic Sampling An isokinetic sampling probe is used for measuring the aerosol concentration at the test section. Isokinetic sampling of aerosols refers to a condition of measurement where the velocity of the free stream is matched exactly with the velocity at the inlet of the probe (Fuchs [2]).

The isokinetic sampling has some errors that studied by series of authors. Lipatov et al. [15] studied experimentally the aspiration of coarse particles by a thin walled sampler. They found that the secondary aspiration after particles have bounced from the outer surface of the sampler is important. Hangal and Klaus (1990) developed a model for the overall efficiency of tubular inlets samplers based on the experimental data that they obtained from wind tunnel. Rosner and Menelaos [16] made correction for sampling errors due to coagulation and wall losses in laminar and turbulent flow. Fan et al. [17] developed an empirical model for the deposition of the particles in the inner wall of the sampling probe.

A specially designed aluminum vacuum tube, which is an upgraded version of the glass one used by Kvasnak et al.[12] is used for concentration measurements at the test section. The inlet of the probe is a 3.81 mm brass tube with a wall thickness of 0.38 mm. A vacuum pump is connected to the bottom half of the probe and provides an appropriate volumetric flow rate to establish the isokinetic environment for the flow velocity at the probe inlet. Figure 2 shows the schematic of the isokinetic sampling.

Injection System The aerosol used in the experiment is generated by an injector driven by a

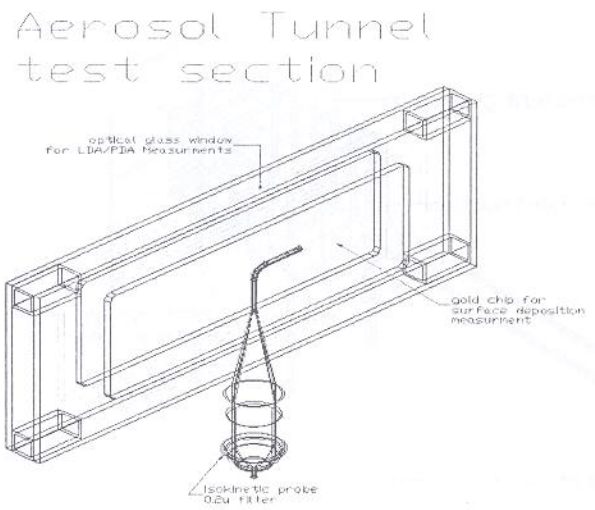

Figure 2. Schematic drawing of the injection system and sampler.

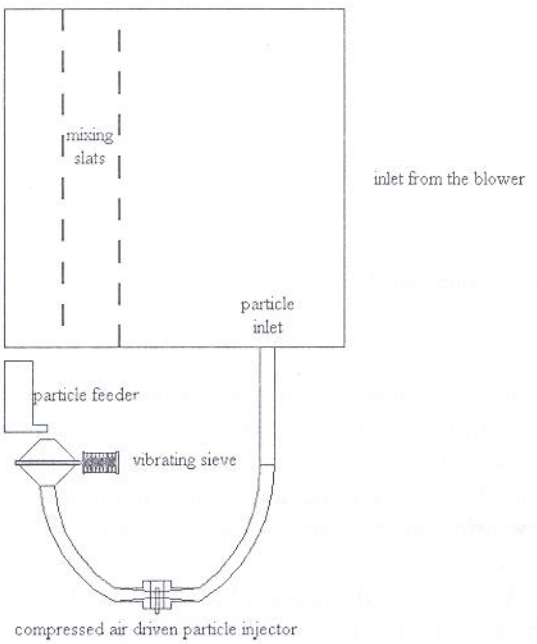

Figure 3. Schematic drawing of the injection of the particles.

compressed air jet which breaks up agglomerates and provides a roughly mono-disperse aerosol of spherical and/or non-spherical solid particles and/or fibers. A Xerox toner feeder and a vibrating sieve provide up to 40 grams per minute steady feed rate of particles. The toner feeder uses a small auger rotating at a constant rate to deliver dust to the sieve. The sieve vibrates and sieves the particles and causing agglomerates to be broken apart. The particles are removed from the sieve and injected into the tunnel using vacuum aspirator driven by compressed air. The compressed air used to drive the injector is filtered to remove moisture and particles down to a size of 0.3 μm. Once the particles in the tunnel are mixed into the flow by a series of slats creating a homogeneous mixture of particles. Figure 3 shows the schematic of the injection system.

Filter and Wall Deposition Surfaces In the experiments, the number of particles deposited on the membrane filter used to capture particles in the isokinetic sampling probe is evaluated. The filter is 37 mm in diameter and has a pore size of 0.2 μm that is not visible at the magnification being used. Another filter is also sticked to the wall in order to measure the particles deposited in the wall. The surface of this filter is rough and is shown in Figure 4.

3. PARTICLE COUNTING

A Scanning Electron Microscope (SEM) in which a beam of electron is scanned over the surface of a solid object and used to build up an image of the details of the surface structure. The SEM that is of the model JSM-6300™ and has a magnification

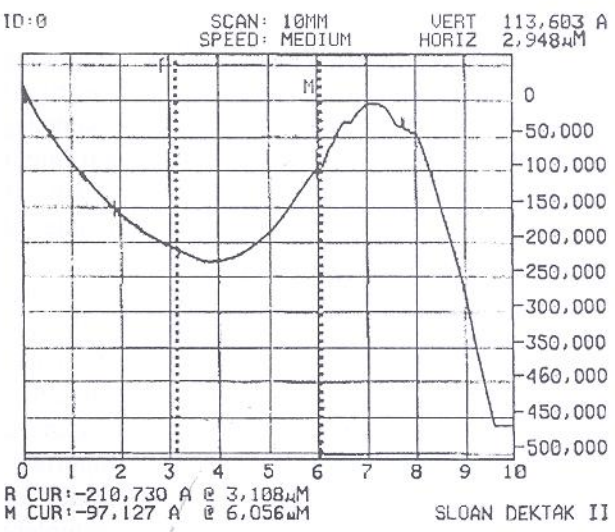

Figure 4. The surface Roughness of the sample.

ability of 300,000, but the amount of the magnification that was used in this research is depend on the particle type and the amount of the particles deposited on the filters. Each image was treated as an independent sample and 100 images were used for obtaining the average deposition rate of particles of different sizes in each sample. The image width and height is between (300 μm-500 μm). The sizing of the particles is done by VOYAGER™ [25] that measures the features in gray-level or binary images of the samples. All the images are converted to binary files. Then each of the separate binary files should be filtered and analyzed separately.

The new and advanced technique for measuring the amount of deposited particles is Image Processing Technique. Figure 5 helps to discuss the image processing technique. Figure 5a shows the original image that is gray format and is taken by an Electron Scanning Microscope. This image is the illustration of spherical particles deposited in the filter of an isokinetic sampler. The image will be ready for processing by converting it to a binary image as it is shown in Figure 5b. This binary image has some defects that should be cleared before processing. The sample edges are not well clear in this image due to electron beam refraction from the object. Also there is one hole in particle that is not realistic (Since the particles are spherical glasses). The defects of this binary image should be cleared before particle counting. VOYAGER™ [25] is used for solving these problems. The images like Figure 5b are filtered by using VOYAGER™ [25]. The filtered image is shown in Figure 5c. Basically, couple of filters is used for making image of Figure 5c. First, the holes in the particles should be filled (step one of filtration), and each particle should be closed (step two), and finally (step three) the particles that are attached to each other after filtration, should be separated.

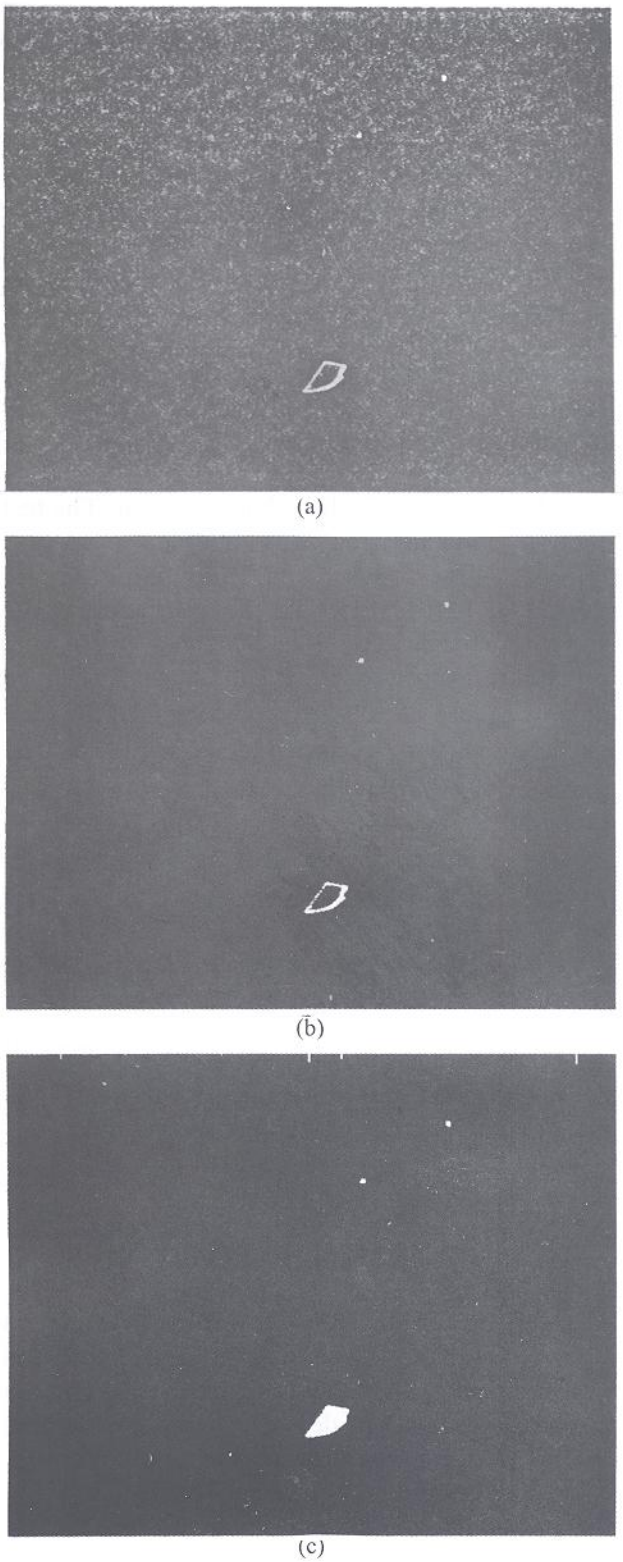

Figure 5. Process for making a suitable image for counting particles.

(a) Grey format image before filtering
(b) Binary format image before filtering
(c) Binary format image after filtering

4. MEASUREMENT PROCEDURE

The inlet tube of the isokenetic probe was placed at the centerline of the tunnel. The vacuum pump was set in a manner that the flow rate into the probe is equal to the flow rate in the channel. A manometer is used to control suction flow rate and a suction

flow rate of 3.75 l/min was needed to sustain a mean velocity of 5 m/s at the probe inlet.

A maximum test section aerosol particle concentration of less than 1% by weight may be used to avoid a significant alteration of the undisturbed turbulent flow field. According to the data reported by Hetsroni (1982), such a concentration may increase the pressure drop by a negligible amount of about 0.2%. Use of higher concentration levels may lead to substantial modification of the structure of turbulence. The aerosol was generated by dispersing approximately 1 g of particle of duration of 10 s. This corresponds to a loading of 0.2%, which is far less than 1% limit. The test section concentration was sampled over a 5 minutes time span, and the particles are deposited in the filter in the isokinetic probe were analyzed by an image processing procedure. Approximately 100 images having an area of square of 300 μm were averaged for each particle size with a bandwidth of $\pm 1.0\mu m$. The mean concentration at the test section C_0 was given by

$$C_0 = \frac{N_f}{A_{image}} \frac{A_{filter}}{A_{probe}} \frac{1}{Vt} \quad (1)$$

where N_f is the average number of particles on the image, A_{image}, A_{filter}, A_{probe} are the areas of the image, filter and probe inlet, respectively, Vis the air velocity at the probe inlet and t is time.

5. DEPOSITION VELOCITY

The average deposition velocity of particles on the filter probe over a 1 min was calculated from the measurement of the number concentration and the number deposition. The deposition velocity is defined as the flux of particles to the wall over the concentration of the free stream. That is

$$u_d = \frac{J}{C_0} \quad (2)$$

where u_d is the deposition velocity, J is the flux of particles to the wall and C_0 is the free stream concentration. It is assumed that the particles deposit uniformly on the channel wall so that any area provides a representative statistical sample. The nondimensional deposition velocity u_d^+ is defined as

$$u_d^+ = \frac{u_d}{u^*} \quad (3)$$

where u* is the friction velocity defined as

$$u^* = \sqrt{\frac{\tau_w}{\rho}} \quad (4)$$

Here, τ_w is the wall shear stress and ρ is the density of the air. In the experiment, the particle flux J (number deposited per unit area per unit time) to the wall was evaluated as

$$J = \frac{N_w}{A_{image} t} \quad (5)$$

where N_w is the number of deposited particles on the wall in an image, and A_{image} is the area under the microscope. From Equations 1 to 4, it follows that

$$u_d^+ = \frac{N_w V A_{probe}}{N_f u^* A_{filter}} \quad (6)$$

Equation 6 implies that the deposition velocity may be calculated directly by counting the number of particles that are deposited on the filter of the isokenetic probe and on the test specimen, and knowing V and u* as well.

6. RELAXATION TIME

The relaxation time is characteristic time scale of particles and is commonly used to correlate experimental data as well as analytical model results.

The nondimensional relaxation time for a sphere is given as

$$\tau_d^+ = \frac{Sd^{+2}}{18} \tag{7}$$

where $d^+ = \frac{du^*}{\nu}$ is the nondimensional particle diameter.

Due to anisotropy of the drag force, for elongated rigid particles, several relaxation times could be defined. Shapiro and Goldenberg (1993) suggested an equivalent relaxation time that is based on the random fiber orientation and the average mobility dyadic. Fan and Ahmadi (1995) used the orientation average translation dyadic instead of mobility dyadic. Soltani and Ahmadi (1995) adopted a similar definition for curly fibers.

Kvasnak and Ahmadi (1995) [13] defined a relaxation time for rigid fibers based on equivalent volume. That is, τ_{vol}^+ is given by Equation 7 with d being replaced by the diameter of the equivalent sphere, given as

$$\tau_{vol}^+ = \frac{Sd^{+2}\beta^{2/3}}{18} = \tau_d^+ \beta^{2/3} \tag{8}$$

Shapiro and Goldenberg (1993) suggested the use of an equivalent relaxation time based on the orientation-averaged resistance for rigid fibers. In this case τ_{eq}^+ is defined as

$$\tau_{eq}^+ = \tau_d^+ \frac{\beta \ln(\beta + \sqrt{\beta^2 - 1})}{\sqrt{\beta^2 - 1}} \tag{9}$$

7. EMPIRICAL MODELS

The experimental results are compared with several empirical models. Wood [18] proposed an empirical equation for particle deposition rates in turbulent flows. His equation is given by

$$u_d^+ = 0.057Sc^{-2/3} + 4.5\times10^{-4}\tau^{+2} + \tau^+ g^+ \tag{10}$$

where Sc is Schmidt number defined by

$$Sc = \frac{\nu}{D} \tag{11}$$

and D is diffusivity of the particle given by

$$D = \frac{\tau}{m} kT \tag{12}$$

Here, τ is the particle relaxation time, m is the mass of particle, k is Boltzmann constant ($k = 1.38\times10^{-23} JK^{-1}$), T is the temperature Kelvin, and g^+ is nondimensional acceleration of gravity.

Fan and Ahmadi (1992) proposed an empirical equation for the rate of deposition of particles in rough surface

$$u_d^+ = \begin{cases} 0.084Sc^{-2/3} + \frac{1}{2}\left[\frac{\left(0.64k^+ + \frac{d^+}{2}\right)^2 + \frac{\tau^{+2}g^+L_1^+}{0.01085(1+\tau^{+2}L_1^+)}}{3.42 + \frac{\tau^{+2}g^+L_1^+}{0.01085(1+\tau^{+2}L_1^+)}}\right]^{1/(1+\tau^{+2}L_1^+)} \\ \times\left[1+8e^{-(\tau^+-10)^2/32}\right]\frac{0.037}{1-\tau^+L_1^+(1+\frac{g^+}{0.037})} & if\ u_d^+ < 0.14 \\ 0.14 & otherwise \end{cases} \tag{13}$$

where the nondimensional lift coefficient is defined as

$$L_1^+ = \frac{3.08}{Sd^+} \tag{14}$$

In Equation 10, g^+ is the nondimensional acceleration of gravity; k+ is the nondimensional roughness ($k^+ = \frac{ku^*}{\nu}$, k is surface roughness). For a horizontal channel, $g^+ = 0$ and the gravitational sedimentation velocity $\tau^+ g^+$ must be

added to Equation 13 for evaluating the total deposition velocity. Shapiro and Goldenberg (1993) proposed several empirical equations for predicting the effect of fiber length on the deposition velocity in vertical and horizontal ducts. Kvasnak and Ahmadi [13] modified Wood's equation along the line of Shapiro and Goldenberg to obtain an improved empirical model for the deposition velocity of straight fibers given as

$$u_d^+ = 4.5\times10^{-4}\tau_e^{+2} + 5\times10^{-3}L^{+2} + \tau_e^+ g^+ \qquad (15)$$

where $L^+ = Lu^*/\nu = d^+\beta$ is the nondimensional particle length. The first term in Equation 15 is the fiber deposition induced by eddy diffusion impaction. The second term is due to the interception mechanism and the third term corresponds to the gravitational sedimentation in horizontal ducts.

Fan and Ahmadi [19] developed a semi-empirical equation for the deposition velocity of spherical particles on smooth and rough surfaces in vertical ducts. Fan and Ahmadi (1997) extended their equation to cover the Brownian diffusion of rigid fibers in turbulent flows. Soltani and Ahmadi (1998) also provided a modified equation for application to curly fiber deposition on smooth surfaces in the absence of gravitational effects and lift force.

Based on the expression for the equivalent relaxation time, Fan and Ahmadi [19] developed the following empirical equation for ellipsoidal particle deposition on smooth surface

$$u_d^+ = \begin{cases} 0.0185\times\left[\dfrac{\beta L^{+2}}{\beta+3} + \dfrac{\dfrac{4\beta\tau_e^{+2}g^+L_1^+}{0.01085(\beta+3)(1+\tau^{+2}l_1^+)}}{3.42+\dfrac{\tau_e^{+2}g^+l_1^+}{0.01085(1+\tau^{+2}L_1^+)}}\right]^{1/(1+\tau^{+2}l_1^+)} \\ \times\left[1+8e^{-(\tau_e^+-10)^2/32}\right]\dfrac{1}{1-\tau_e^+L_1^+(1+\dfrac{g^+}{0.037})} & if\ u_d^+ < 0.14 \\ 0.14 & otherwise \end{cases} \qquad (16)$$

where the nondimensional lift coefficient is defined as

$$L_1^+ = \frac{3.08}{Sd_{eq}^+} = \frac{0.725}{\sqrt{S\tau^+}} \qquad (17)$$

for $\beta = 1$, Equation 16 reduces to the empirical equation for spherical particles. In Equation 16, g^+ is the nondimensional acceleration of gravity. For a horizontal channel, $g^+ = 0$ and the gravitational sedimentation velocity $\tau^+ g^+$ must be added to Equation 16 for evaluating the total deposition velocity.

Shams and et al. [20] developed an empirical model for flexible fibers. Their model is for flexible fibers that initially released in the flow direction are developed. This model is function of equivalent relaxation time, aspect ratio and diameter. The deposition velocity of flexible fibers in the sidewalls of a channel is related as

$$u_d^+ = \begin{cases} 0.0234\times\left[\dfrac{\beta L^{+2}}{\ln(\beta)+3} + \dfrac{0.9e^{d^{+2}}}{(\ln(\beta)+1)e^{(\tau_d^+-1)^3}}\right] \\ \times\left[\dfrac{1+10e^{-(\tau_d^+-13)^2/32}}{0.049\beta^{2.5}+10}\right] & if\ u_d^+ < 0.14 \\ 0.14 & otherwise \end{cases} \qquad (19)$$

It will be shown that the model prediction is well comparable with the numerical simulations at various conditions of flow and fiber properties.

8. RESULTS

Deposition rates of particles are studied by using an experimental setup. Dispersion for three classes of particles, namely, spherical glass particles with diameter of 1-30 μm, and irregular shapes, and fibrous particles are studied and deposition velocity of spherical particles with surface roughness is measured.

(a)

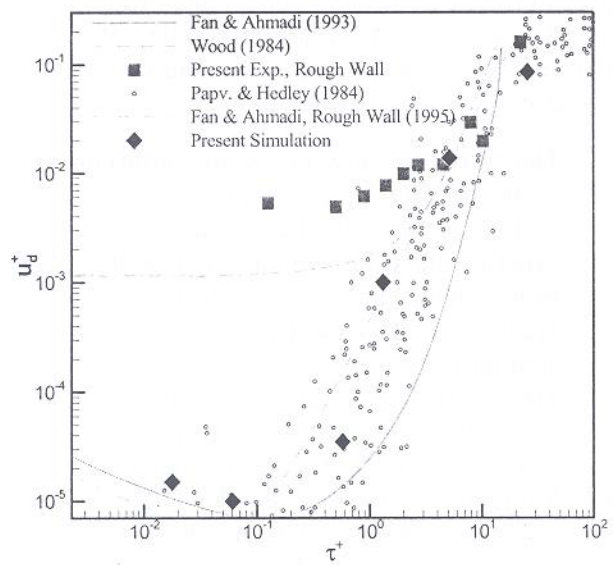

(b)

Figure 6. Spherical particles processing.
(a) Spherical particle image
(b) Dimensionless deposition velocity versus dimensionless relaxation time for spherical particles

The particle concentration at the test section was measured with the aid of an isokenetic probe. The image processing technique is used to count the amount of deposited particles.

9. SPHERICAL PARTICLES

Figure 6a shows one sample of the deposited particles on the surface of the wind tunnel. The Deposition rates of glass particles of 5-40 μm are measured for a flow Reynolds number of 15000 and are presented in Figure 6b.

The particle to fluid density ratio is approximately 2000 and the non-dimensional shear velocity is 0.3. The roughness value that is used here is 30 μm. The results are presented in terms of non-dimensional deposition velocity versus non-dimensional relaxation time.

The results are compared in the figure with the available experimental data of Papvergos and Hedley [21], empirical model of Wood [18] and the empirical model of Fan and Ahmadi (1995) that includes the effect of roughness. This figure shows that the roughness has a significant effect on small particle deposition as it was also predicted by Fan and Ahmadi (1995) empirical model.

These results show that the deposition velocity increases as particle diameter increases (or by increasing non-dimensional relaxation time).

10. IRREGULAR SHAPED PARTICLES

One sample of deposited irregular shaped particles on the sidewall of the wind tunnel is shown in Figure 7a. The dimensionless deposition velocity of irregular shaped particles is shown with respect to dimensionless relaxation time in Figure 7b.

The results are compared in the figure with the simulation of Fan and Ahmadi [19] with and without roughness and empirical model of Wood [18]. The experimental data of Papvergos and Hedley [21] are also shown in the figure for comparison. These results show that the irregular shaped particles have a higher deposition velocity as compared with spherical one. The reason for this deposition efficiency is the higher drag force with respect to spherical particles. The

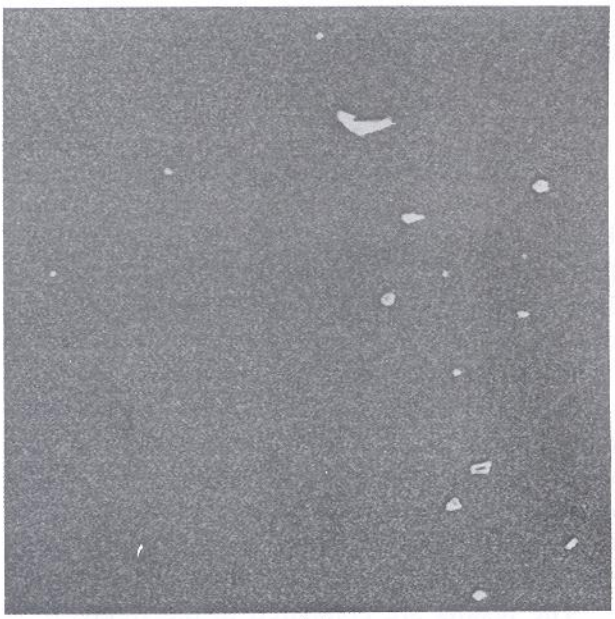

(a)

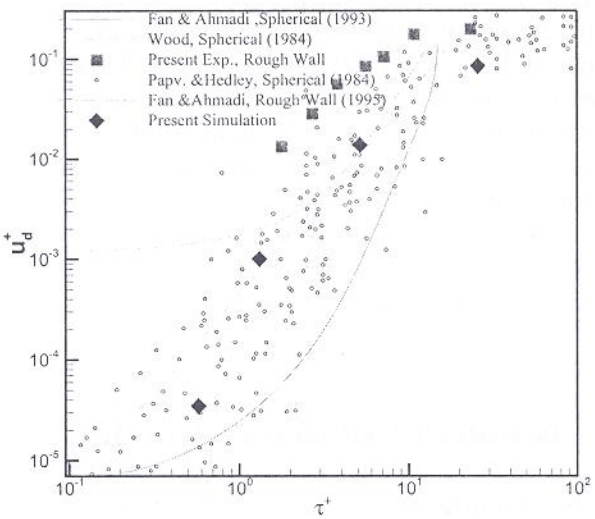

(b)

Figure 7. Irregular shaped particles processing.
(a) Irregular shaped particle image
(b) Dimensionless deposition velocity versus dimensionless relaxation time for irregular shaped particles

roughness has a tremendous effect on small particles ($\tau^+<7$). The results show that the roughness effects on big particles are negligible ($\tau^+>10$).

11. RIGID FIBERS

Sample deposition of rigid fibers on the sidewall of the wind tunnel is shown in Figure 8. The fibers are made from glass Silicon and the lengths are in the range of 2-30 μm. The dimensionless velocities will be presented in the future works. The fibers were coagulated due to electrostatic charging. The authors will investigate the effect of this charging in future.

12. CONCLUSION

An experimental simulation of particle transport and deposition in a turbulent flow is performed. The experiments have done with the use of a turbulent two-phase wind tunnel. The experimental results for rough surface are compared with the available experimental data and the earlier simulation studies for horizontal ducts. Based on the presented results, the following conclusions are drawn:

1. The turbulent flow plays an important role on the particle deposition process.
2. Comparison of the results with the experimental data and earlier modeling effort shows that using the proposed approach for evaluating the particle deposition is a reasonable approach.
3. The deposition velocity in the inertia range is a function of particle relaxation time and increases as particle diameter increases.
4. In the diffusion range, the deposition velocity increases as particle diameter decreases.
5. The rough surface deposition or deposition velocity is higher than the smooth surface deposition.
6. Electrostatic charging during fiber injection is the dominant deposition mechanism.

13. LIST OF SYMBOLES

1. Area of filter A_{filter}
2. Area of image A_{image}
3. Cross section of probe A_{probe}

4. Particle concentration C_0
5. Empirical constants $C_D, C_\mu, C_{1\varepsilon}, C_{2\varepsilon}$
6. Couningham constant C_c
7. Particle diameter d
8. Diffusion flux D
9. Gravitational acceleration g
10. Channel height h
11. Near wall particle flux J
12. Fiber length L
13. Deposited number of particles on image N_f
14. Deposited number of particles on the walls N_w
15. Time t
16. Shear velocity u*
17. Dimensionless velocity of particle u^{p+}, v^{p+}, w^{p+}
18. Velocity in the probe V_t
19. Velocity vector in fiber v_I
20. Position vector of fiber x_i

Greek Letters

Distance between coherent vortices	Λ^+
Aspect ratio	β
Kroneker delta	δ
Fluid viscosity	μ
Fluid kinematic viscosity	ν
Mean free path	λ
Solid phase density	ρ_p
Fluid density	ρ_f
Effective relaxation time	τ_e
Relaxation time based on diameter	τ_d
Relaxation time based on volume	τ_v
Rigid fibers volumetric relaxation time	τ^+_{vol}
Rigid fibers equivalent relaxation time	τ^+_{eq}

14. REFERENCES

1. Cooper, D. W., "Particle Contamination and Microelectronics Manufacturing: An Introduction", ***Aerosol Sci. Technol.***, Vol. 5, (1986), 983-992.
2. Fuchs, N. A., "The Mechanics of Aerosol", Pergoman Press, London, (1964).
3. Friedlander, S. K., "Smokes, Dust, and Haze", John Wiley, New York, (1977).
4. Hinds, W. C., "Aerosol Technology, Properties Behavior, and Measurement of Airborne Particles", John Wiley and Sons, New York, (1982).
5. The Turbulent Case. ***J. Aerosol Sci.***, Vol. 19, (1982), 197-211.
6. Hedley, G. M., "Aerosol, An Industrial and Environmental Science", Academic Press, New York, (1984).
7. Vincent, J. H., "Aerosol Science for Industrial Hygienists", Pergoman, Oxford, (1996).
8. Wells, M. R. and Chamberlain, A. C., "Deposition of Dusts from Turbulent Gas Streams" ***Atm Environment***, Vol. 3, (1969), 494-496.
9. Namie, S. And Ueda, T., "Droplet Transfer in Two-Phase Annular Mist Flow. Part I: Experiment of Droplet Transfer Rate and Distribution of Droplet Concentration and Velocity", ***Bull. JSME***, Vol. 15, (1972), 1568-1580.
10. McCoy, D. D. and Hanratty, T. J., "Rate of Deposition of Droplets in Annular Two Phase Flow" ***Int. J. Multiphase Flows***, Vol. 3, (1977), 275-295.
11. Montgomery, T. L., "Aerosol Deposition in a Pipe With Turbulent Air Flow", D.Sc. Dissertation, University of Pittsburgh, (1969).
12. Kvasnak, W., Ahmadi, G., Bayer, R. and Gaynes, M., "Experimental Investigation of Dust Particle Deposition in a Turbulent Channel Flow", ***J. Aerosol Sci.***, Vol. 25, (1993), 795-815.
13. Griffiths, W. D. and Vaughan, N. P., "The Aerodynamic Behavior of Cylindrical and Spheroidal Particles When Settling Under Gravity", ***J. Aersol Sci.***, Vol. 17, (1986), 53-65.
14. Shapiro, M. and Goldenberg, M., "Deposition of Glass Fiber Particles from Turbulent Flow in Pipe", ***J. Aersol Sci.***, Vol. 24, (1993), 53-65.
15. Kvasnak, W. and Ahmadi, G., "Fibrous Particle Deposition in a Turbulent Channel: An Experimental Study", ***Aerosol Sci. And Tech.***, Vol. 23, (1995), 641-652.
16. Gayne, J. C., "Experimental Investigation of Particle Deposition and Effect of Rebound in a Turbulent Channel Flow", M.Sc. Dissertation, Clarkson University, (1998).
17. Lipatov, G. N., Grinspun, S. A., Shingaryov, G. L. and Sutugin, A. G., "Aspiration of Coarse Aerosol by a Thin-Walled Sampler", ***J. Aerosol Sci.***, Vol. 17, (1986), 763-769.
18. Rosner, D. and Tassopoulos, M., "Correction for Sampling Errors Due to Coagulation and Wall Loss in Laminar and Turbulent Tube Flow: Direct Solution of Canonical 'Invers' Problem for Log-Normal Size Distribution", ***J. Aerosol Sci.***, V. 22, (1991), 843-867.
19. Fan, B. J., Wong, F. S., McFarland, A. R. and Anand, N. K., "Aerosol Deposition in Sampling Probe", ***Aerosol Sci. Tech.***, V. 17, (1992), 326-332.
20. Wood, N. B., "The Mass Transfer of Particles and Acid Vapor to Cooled Surfaces", ***J. Inst. Energy***, Vol. 76, (1981), 76-93.
21. Fan, F. G., and Ahmadi, G., "A Sublayer Model for Turbulent Deposition of Particles in Vertical Ducts With

Smooth And Rough Surfaces," ***J. Aerosol Sci.***, Vol. 24, (1993), 45-64.
22. Shams, M., Ahmadi, G. and Rahimzadeh, H., "Dispersion and Deposition of Flexible Fibers inTurbulent Duct Flows", ***J. Aerosol Sci.***, to be published.
23. Papavergos, P. G. and Hedley, A. B., "Particle Deposition Behavior From Turbulent Flows," ***Chem. Eng. Des.***, Vol. 62, (1984), 275-295.
24. Sehmel, G. A., "Particle Eddy Diffusivity and Deposition Velocities for Isothermal Flow and Smooth Surfaces," ***J. Aerosol Sci.***, Vol. 4, (1973), 125-138.
25. Sun, Y. F. and Lin, S. P., "Aerosol Concentration in a Turbulent Flow" ***J. Colloid and Interface Sci.***, Vol. 113, (1986), 315-320.
26. Rosner, D. and Tassopoullos, M., "Correction for Sampling Errors Due to Coagulation and Wall Loss in Laminar and Turbulent Tube Flow: Direct Solution of Canonical 'Inverse' Problem for Log-Normal Size Distribution" ***J. Aerosol Sci.***, Vol. 22, (1986), 843-867.
27. VOYAGER, Technical Manual, Clarkson University.
28. JSM-6300, Technical Manual, Clarkson University.
29. Fan, F. G., "A Sublaryer Model for Wall Depositions of Ellipsoidal Particles in Turbulent Streams", ***J. Aerosol Science***, Vol. 26, (1995), 813-840
30. Soltani, M. and Ahmadi, G., "Direct Numerical Simulation of Particle Entertainments in Turbulent Channel Flow", ***Phys. Fluids***, Vol. 7, (1995), 647-657.
31. Hangal, S. and Klaus, W., "Overall Efficiency of Tubular Inlets Sampling at 0-90 Degrees from Horizontal Aerosol Flows", ***Atoms. Env.***, Vol. 24A, (1990), 2379-2386.
32. Stavropoulos, N., Columbia University, MSc Thesis, New York, (1957).